FEBS 18857 FEBS Letters 412 (1997) 15–20

The conformational preference of gramicidin channels is a function of lipid bilayer thickness

Niloufar Mobashery, Claus Nielsen, Olaf S. Andersen*

Department of Physiology and Biophysics, Cornell University Medical College, 1300 York Avenue, New York, NY 10021, USA

Received 19 May 1997

Abstract In order to understand how the material properties of lipid bilayers could affect integral membrane protein function, we examined the effect of a hydrophobic mismatch on the structure and function of membrane-spanning gramicidin channels. Changes in lipid bilayer thickness affect the conformational preference of membrane-spanning gramicidin A (gA) channels (single–stranded [SS] dimers ↔ double-stranded [DS] dimers) and induces an additional conductance state in the standard (SS) $\beta^{6.3}$-helical channel. These results provide experimental evidence for the importance of energetic coupling between the bilayer and imbedded inclusions.

Key words: Hydrophobic matching; Membrane deformation energy; Single stranded channel; Double stranded channel

1. Introduction

There is abundant evidence that the function of integral membrane proteins is affected by the membrane lipid composition [1,2]. Within the framework of the fluid mosaic model [3], the cell membrane has often been approximated as a thin sheet of liquid hydrocarbon in which integral proteins are imbedded. In this context the membrane influence on protein function has been attributed to changes in bilayer fluidity (viscosity). It is increasingly recognized, however, that fluidity per se cannot be a major factor in regulating protein function [4–6]. An alternative point of view has focused on the liquid-crystalline properties of the lipid bilayer matrix [7], which leads to the notion that the material properties of the bilayer (thickness, monolayer curvature and bilayer stress) are important for membrane protein function [8–14]. The underlying mechanisms remain obscure, except that quaternary conformational changes in the membrane-spanning domain of integral membrane proteins will cause reciprocal changes in the structure of the surrounding bilayer [10–14]. The associated membrane deformation energy will be a component of the overall free energy of the protein conformational change. In order to obtain further insight into this question it is important to have information about the effect of membrane lipids on systems that undergo a well-defined conformational change, such as the monomer–dimer transition of the channel-forming gramicidin (gA) molecules.

gA are miniproteins, formed by two monomers that have the sequence: [15] Formyl-L-Val–Gly–L-Ala–D-Leu–L-Ala–D-Val–L-Val–D-Val–L-Trp–D-Leu–L-Trp–D-Leu–L-Trp–D-Leu–L-Trp–ethanolamine and the structure of gA channels is known at atomic resolution [16]. The standard gA channels are formed by the formyl-NH-to-formyl-NH transmembrane association of single-stranded (SS) $\beta^{6.3}$-helical monomers (Fig. 1a) from the two monolayers: the channels form preferentially when gA is added to both sides of the bilayer [17] (see [18] for a review of gA channels).

Under most experimental conditions gA channels have this single well-defined structure [19–21], which differs from the structures of gA in organic solvents, where gA occurs as a mixture of monomers and different double-stranded (DS) helical dimers [22]. Normally DS gA dimers (Fig. 1b) do not form membrane-spanning channels [18]; some combinations of gA analogues do form DS channels, however [23]. When that is the case, channel activity occurs after gramicidin addition to either one or both sides of the bilayer.

At high gA/lipid molar ratios ($>1/50$) a hydrophobic mismatch between gA channels length and membrane thickness causes a lamellar $\rightarrow H_{II}$ phase transition in dioleoylphosphatidylcholine (di-$C_{18:1}$-PC) bilayers [24], because of a build-up of mechanical stress in the bilayer which is relieved by the lamellar $\rightarrow H_{II}$ phase transition [25]. The hydrophobic mismatch will not only affect the membrane lipids but will also affect the conformational equilibrium of the membrane-spanning gA dimers. Given the existence of multiple gA conformers in organic solvents, this raises the possibility that one could obtain direct evidence for the functional and structural importance of a hydrophobic mismatch between membrane proteins (in casu gA channels) and the host bilayer. Specifically, the equilibrium distribution between SS and DS channels is likely to vary as a function of membrane thickness. An increase in membrane thickness, which will increase the mismatch between channel length and membrane thickness, is expected to have a larger destabilizing effect on formyl-NH-to-formyl-NH SS dimers than on intertwined DS dimers.

2. Materials and methods

Di-$C_{18:1}$-PC, dieicosenoylphosphatidylcholine (di-$C_{20:1}$-PC), and dierucoylphosphatidylcholine (di-$C_{22:1}$-PC) were from Avanti Polar Lipids (Alabaster, AL). *n*-Decane was from Wiley Organics (Columbus, OH). gA, [Ala^{0b}–D-Ala^{0a}]gA and [Ala^{0b}–D-Ala^{0a}]gC were gifts from Drs. Roger E. Koeppe II and Gwendolyn Mattice (Department of Chemistry and Biochemistry, University of Arkansas). The gramicidins were dissolved in ethanol (200 proof, U.S. Chemicals, Tuscola, IL) or DMSO (Sigma, St. Louis, MO). Hydrochloric acid (1.0 N) was from Malinckrodt Chemical Works (Paris, KY); electrolyte solutions were prepared daily using deionized Milli-Q water (Milipore Corp, Bedford, MA).

Planar lipid bilayers were formed from a solution of lipid/*n*-decane (2–3% wt/vol) across a 1.6 mm diameter hole in a teflon partition separating two teflon chambers, each containing 5 ml of 0.1 M

*Corresponding author. Fax: +1 (212) 746-8690.
e-mail: sparre@med.cornell.edu

This work has already appeared in abstract form: C. Nielsen, Mobashery, N. and Andersen, O.S., Biophys. J., 72:A191.

PII S0014-5793(97)00709-6

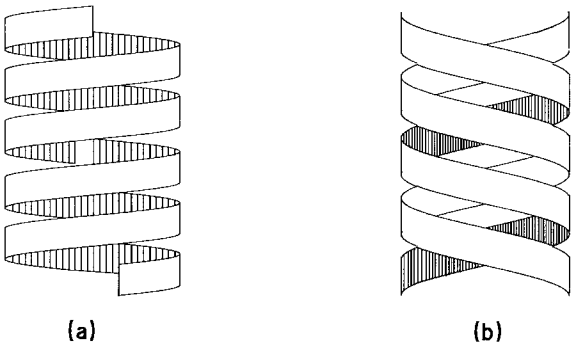

Fig. 1. Structures of gA dimers: (a) SS dimers and (b) DS gA dimers.

HCl. The temperature was maintained at 25±1°C. Aliquots of gA dissolved in either ethanol or DMSO were added to one (asymmetrical addition) or both (symmetrical addition) aqueous phases during stirring.

The bilayer punch [26] was used to isolate a small membrane patch (30 μm pipette diameter). Channel activity was recorded at 200 mV using an Axopatch-1B amplifier (Axon Instruments, Foster City, CA). The current signal was filtered (f_c = 500–1000 Hz, −3 dB) with an 8-pole Bessel filter (Frequency Devices, Haverhill, MA) before input to an A/D converter in a PC/AT-compatible 80486 computer. The signal was digitized at 5 times the filter frequency and transitions were detected off-line using PClamp6 (Axon Instruments). The curves in the dwell time histograms denote the fit of single exponential distributions of the results using a simplex least squares method. In order to display the long (9 min) current traces that are needed to describe the results (Fig. 2a–c, Fig. 3a, Figs. 4a, and 5), data compression is used. For every set of 10 consecutive current values in the digitized data, mean and standard deviation (S.D.) values are computed. From the subset

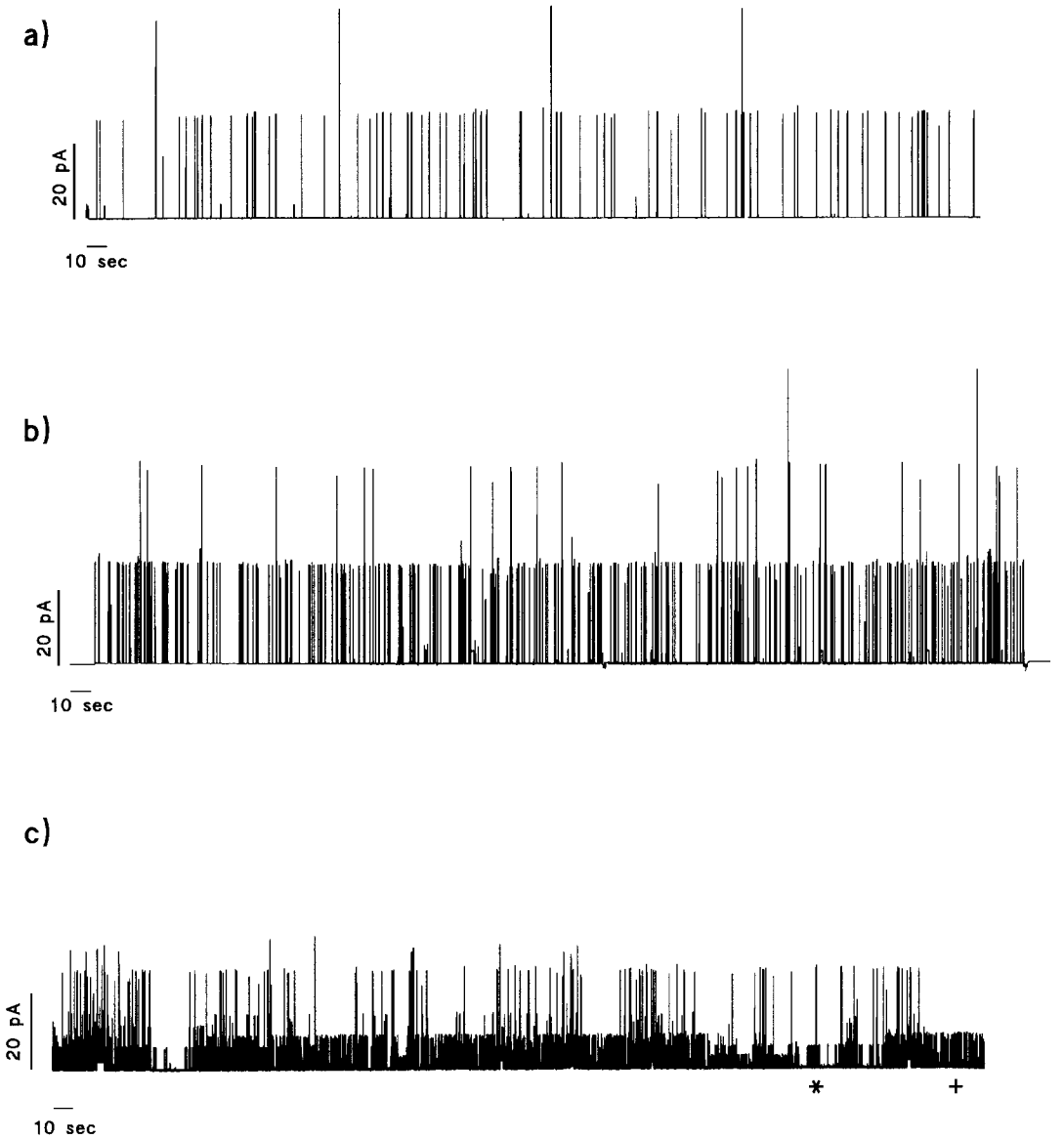

Fig. 2. Current transitions observed when gA (dissolved in ethanol) is added to both sides of bilayers formed by phosphatidylcholines having different acyl chain length. (a) gA channel activity in di-$C_{18:1}$-PC bilayers. The 9 min current trace shows 25 pA transitions rising from baseline. On a few occasions, two gA channels are open simultaneously, which gives rise to a total current of 50 pA. Mean dwell time is 140 ms. (b) Same as (a) except that the bilayer was formed by di-$C_{20:1}$-PC. Up to 3 concurrent 25 pA gA channels are active in this recording. Mean dwell time is 72 ms. (c) gA channel activity in di-$C_{22:1}$-PC bilayers. The maximal current levels are comparable with those seen in (a) and (b), but other kinds of channel activity are clearly present. For all recordings f_c = 500 Hz, (−3 dB).

of values in each set that fall within the mean ± S.D., a new mean value was calculated. This new mean current value is taken to represent the set of 10 data points.

3. Results

Fig. 2a–c shows gA channel current traces in bilayers formed by di-$C_{18:1}$-PC, di-$C_{20:1}$-PC, and di-$C_{22:1}$-PC. When gA is incorporated into di-$C_{18:1}$-PC or di-$C_{20:1}$-PC bilayers (Fig. 2a,b), there is a single predominant channel type—the standard SS $\beta^{6.3}$-helical channel [27]. In di-$C_{22:1}$-PC bilayers (Fig. 2c), the channel behaviour changes profoundly. There are several different channel types, some of which appear as series of repetitive transitions from the baseline to one or more conducting levels and back to the baseline. A given pattern of activity is seen for extended periods (from seconds to minutes), with abrupt transitions from one type of activity to another. Two types of activity predominate; they are labeled by '*' and '+' in the current traces in Fig. 2c. These types of activity or channel types were seen in more than 20 separate experiments on different days. Other channel types also are observed; they occur less frequently than those in Fig. 2c and will not be discussed further. In addition, we note that the amount of gA that needed to be added in order to observe a given channel activity increases approximately 10-fold every time the acyl chain length is increased by two CH_2 groups.

Both channel types (* and +) were seen when gA was dissolved in ethanol (where gA is present as monomers and DS dimers [28]). Bursts of activity were separated by long periods (up to several minutes) of quiescence. The channels labeled '*' were seen only when gA was added to both sides of the bilayer (or several hours after asymmetric gA addition to only one side of the bilayer). When gA is dissolved in dimethylsulfoxide (DMSO), where gA is monomeric [29], this is the predominant channel type (results not shown). We conclude that these channels are SS dimers; they are described further in Fig. 3. The channels labeled '+' were seen immediately (less than 1 min) upon addition of gA dissolved in ethanol (or several hours after addition of gA dissolved in DMSO), irre-

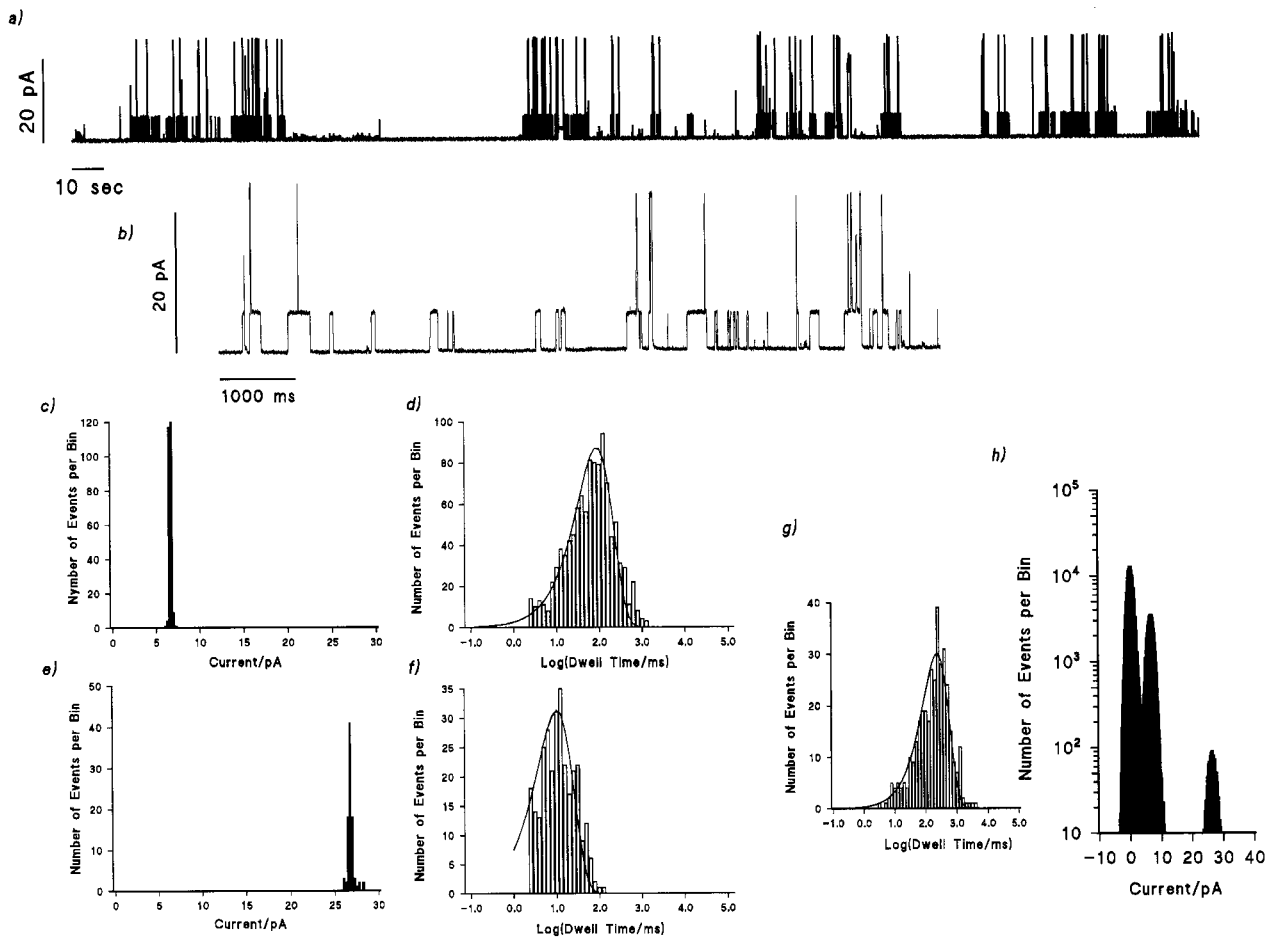

Fig. 3. Analysis of the dominant gA channel activity in di-$C_{22:1}$-PC bilayers. This channel activity is the one labeled '*' in Fig. 2c. (a) When gA was dissolved in DMSO, this channel type could be studied in isolation. Bursts of activity alternate with sustained periods of quiescence in this 9 min current trace ($f_c = 500$ Hz). (b) Segment of the current trace shown in (a) at higher time resolution ($f_c = 500$ Hz) reveals that the maximal conductance state is reached only via an intermediate current level. (c,d) Current transition amplitude histogram and dwell-time histogram for the intermediate current level. The mean current amplitude is 6 pA; the mean dwell time is 88 ms. (e,f) Current transition amplitude histogram (referred to the baseline) and dwell-time histogram for the maximal current level. The mean current amplitude is 27 pA; the mean dwell time is 10 ms. (g) All-points current level histogram obtained from the trace shown in (b). Intermediate (6 pA) and maximal (27 pA) conductance levels are present. Levels corresponding to 27 pA-6 pA = 21 pA or n·6pA, $n = 1,2,...$ are absent. If the 6 pA events were statistically independent, one would expect a peak at 12 pA with a peak count of about 800 which would be readily discernible.

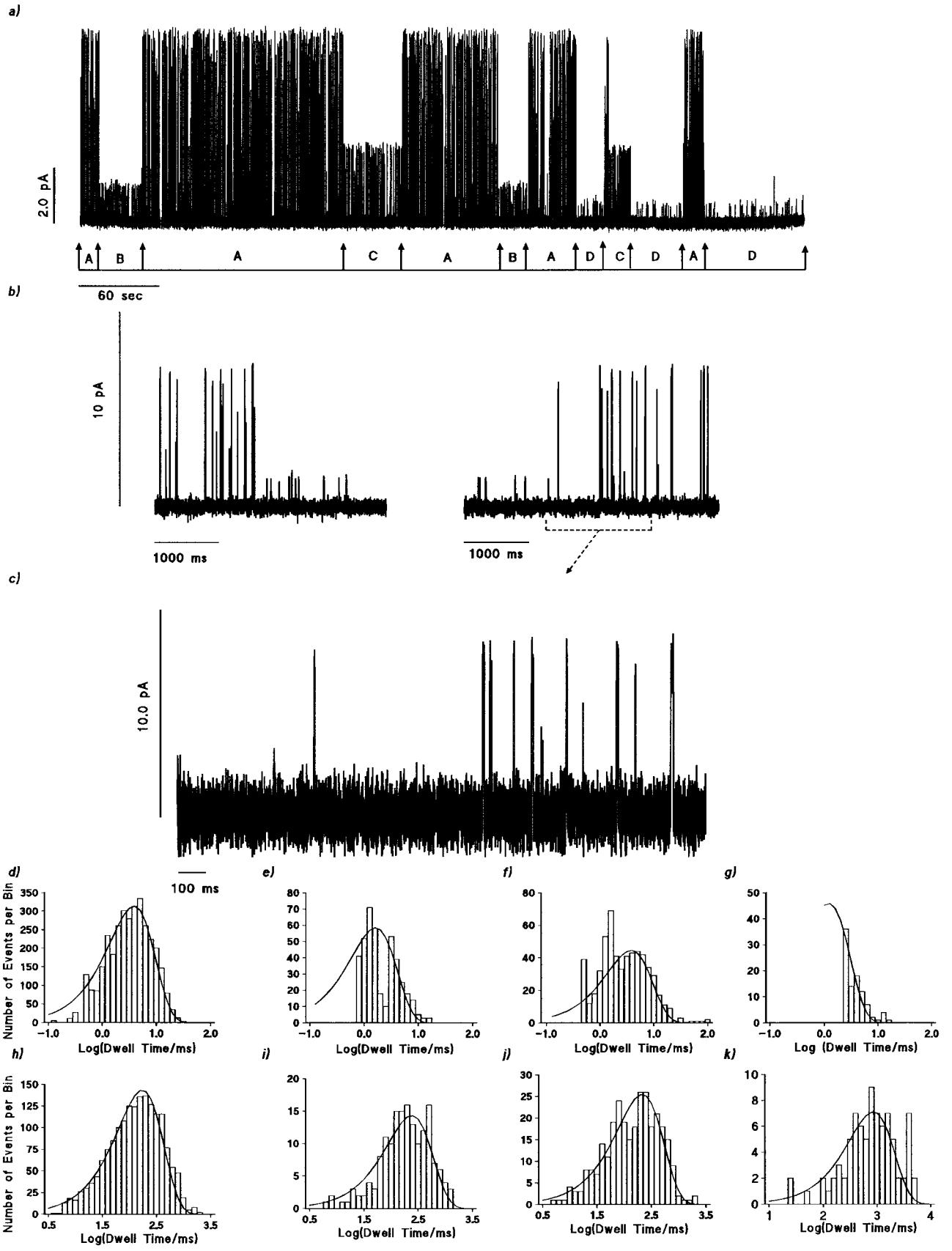
a)
2.0 pA
A B A C A B A D C D A D
60 sec
b)
10 pA
1000 ms
1000 ms
c)
10.0 pA
100 ms
d)
e)
f)
g)
Number of Events per Bin
Log(Dwell Time/ms)
h)
i)
j)
k)

Fig. 4. Analysis of the gA channel activity in di-$C_{22:1}$-PC labeled '+' in Fig. 1c. (a) When gA is dissolved in ethanol and added to one side of the bilayer only, this type of activity is studied in isolation. Four different current levels marked A through D are present, as shown in this 9 min sample trace (f_c = 500 Hz). (b) In the time-expanded trace (f_c = 500 Hz), the abrupt nature of the activity change is visible. The apparent low current states that are seen after onset of the high current activity is due to the limited time resolution of the recording system. When the current trace is digitized and filtered at higher frequencies (f_c = 1000 Hz), the amplitude of these apparently low current states increases.
←

spective of whether gA was added symmetrically or asymmetrically (results not shown). We conclude that these channels are DS dimers; they are described further in Fig. 4.

The events labeled '*' in Fig. 2c are shown at higher resolution in Fig. 3. The lower current trace in Fig. 3b shows two different types of current transitions: transitions from the baseline to a relatively long-lived, intermediate current level, and very brief transitions from the intermediate level to a current level that is indistinguishable from that of standard gA channels in di-$C_{18:1}$-PC and di-$C_{20:1}$-PC bilayers. The amplitude transition histograms and duration histograms for the two current levels are shown in Fig. 3c–f. The all-point current level histogram (Fig. 3g), which depicts the amount of time that is spent at any current level, has only 3 major peaks corresponding to the baseline, the intermediate current level (≈6 pA), and the high level (≈27 pA). Peaks corresponding to multiple levels, or combinations of the intermediate (≈6 pA) and the high level (≈21 pA), are absent. The lack of simultaneous presence of two or more 6 pA events shows that each burst of activity (lasting several seconds) corresponds to repeated association and dissociation between the same two gA monomers. The presence of only these 3 current levels show that the current transitions from the intermediate to the high level (and back) represent conductance changes in a membrane-spanning gA dimer, as opposed to the existence of two different channel types (with current transitions of 6 and 21 pA, respectively).

The current events labeled '+' in Fig. 2c are shown at higher resolution in Fig. 4a, which is part of a longer segment displaying transitions among 4 different kinds of channel activity. The transitions between two different kinds of activity are abrupt, with no evidence for the appearance of the new activity before the old one has ceased (Fig. 4b,c). The open and closed time histograms of the current transitions marked A, B, C D, are shown in Fig. 4d–k. Given the quite different current transition amplitudes, the duration and interval distributions are remarkably similar. These results indicate that we are dealing in each case with kinetically uniform sets of events.

The above results show that the gA channel behavior can be altered qualitatively by altering the membrane thickness. Such changes in channel behavior could be due to the increased lipid bilayer thickness per se or to the increased mismatch between channel length and membrane thickness (cf. [30]). To distinguish between these possibilities, we used the sequence-extended 17-amino-acid gA analogues [Ala^{0b}–D-Ala^{0a}]gA and [Ala^{0b}–D-Ala^{0a}]gC [31], which forms channels that are ≈3.2 Å longer than those formed by gA itself. With [Ala^{0b}–D-Ala^{0a}]gA and [Ala^{0b}–D-Ala^{0a}]gC we see no qualitative changes in channel behavior as the phospholipid acyl chain length is increased from 20 to 22 carbon atoms (Fig. 5). We conclude that the changes in gA channel behavior are due to the mismatch between membrane thickness and channel hydrophobic length—in agreement with the results of Killian et al. [30].

4. Discussion

The conformational preference of gA channels is affected by a hydrophobic mismatch between the host bilayer and the imbedded channel. This result complements the studies of Greathouse et al. [32], who showed that the conformational preference of gA is altered when the acyl chain length of the surrounding phospholipids is much less than that of a $\beta^{6.3}$-helical monomer. Again the hydrophobic mismatch causes DS dimers to form. Together, our results and those of Greathouse et al. show that it is the magnitude of the mismatch (the membrane deformation energy) that is important, which may provide insights into the well-known effects of membrane thickness on the function of integral proteins (e.g., [33]).

Our results can be understood by noting that the free energy difference between gramicidin different configurations (SS monomers, SS dimers, DS dimers) is comprised of contributions from the gramicidin per se and from its interactions with the environment: $\Delta G = \Delta G_{int} + \Delta G_{def}$. The extrinsic contribution to the free energy difference ΔG_{def} for the gA (SS monomer) ↔ (SS dimer) equilibrium will increase with increasing membrane–channel mismatch, as evident from the increased gA concentration needed to observe a given (time-averaged) channel activity in the thicker bilayers. The interfacial gA concentration, therefore, is much higher in di-$C_{22:1}$-PC than in di-$C_{18:1}$-PC or di-$C_{20:1}$-PC bilayers, which will shift the (SS monomer) ↔ (DS dimer) equilibrium in favor of the DS dimers and cause conducting DS channels to appear in the thicker bilayers.

The increased membrane–channel mismatch not only alters the equilibrium distribution among different gA configurations, it also alters the qualitative behavior of SS gA channels

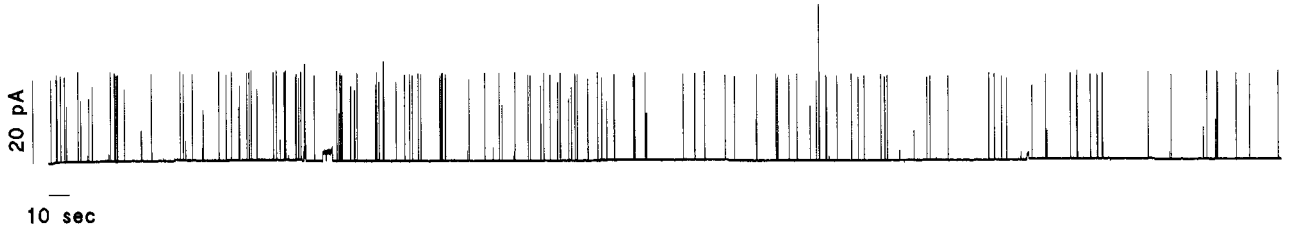

Fig. 5. Channel activity seen after symmetrical addition of [Ala^{0b}–D–Ala^{0a}]gC dissolved in ethanol to di-$C_{22:1}$-PC bilayers. The 9 min continuous current trace shows no evidence for the 'aberrant' gA activity observed in di-$C_{22:1}$-PC bilayers (f_c = 500 Hz).

(Figs. 2c and 3) by introducing a new conducting state and by causing repetitive channel formation by the same two monomers. We do not fully understand the molecular basis for the former effect, but the latter result suggests that the membrane $\beta^{6.3}$-helical monomers are restricted in their lateral motion which could arise because membrane-adsorbed (unfolded) gA monomers form extended rafts. In support of this suggestion, we note that Huang [34] has shown that there is a slight preference for membrane-adsorbed (α-helical) peptides to organize into structures where the helices are separated by a few lipid molecules to give a helix–helix distance of about 40 Å.

Acknowledgements: This work was supported by NIH grant GM21342 (O.S.A.) and Danish Research Council (SNF) grant J-11-1219-1 to C.N. We thank Drs. D.V. Greathouse, R.E. Koeppe II and G.L. Mattice for the gramidicins used in this study, and Drs. H.W. Huang and Koeppe for helpful discussions.

References

[1] Devauex, P.F. and Seigneuret (1985) Biochim. Biophys. Acta 822, 63–125.
[2] Bienvenüe, A. and Marie, J.S. (1994) Curr. Topics Membranes 40, 319–354.
[3] Singer, S.J. and Nichols, G.L. (1972) Science 175, 720–731.
[4] McNamee, M.G. and Fung, T.M. (1988) in: Lipid Domains and the Relationship to Membrane Function (R.C. Aloia, C.C. Curtin, and L.M. Gordon, Eds.), pp. 43–62, Alan R. Liss, New York.
[5] Lee, A.G. (1991) Prog. Lipid Res. 30, 323–348.
[6] Lundbæk, J.A. and Andersen, O.S. (1994) J. Gen. Physiol. 104, 645–673.
[7] Helfrich, W. (1973) Z. Naturforsch. 28c, 693–703.
[8] Gruner, S.M. (1985) Proc. Natl. Acad. Sci. USA 82, 3665–3669.
[9] Huang, H.W. (1986) Biophys. J. 50, 1061–1070.
[10] Mouritsen and Bloom, M. (1984) Biophys. J. 46, 141–153.
[11] Gruner, S. (1991) in: Biologically Inspired Physics (Peliti, L., Ed.), pp. 127–135, Plenum Publishing Corp., New York.
[12] Andersen, O.S., Sawyer, D.B. and Koeppe II, R.E. (1992) in: Biomembrane Structure and Function (Gaber, B.P. and Easwaran, K.R.K., Eds.), pp. 227–244, Adenine Press, Schenectady, NY.
[13] Brown, M.F. (1994) Chem. Phys. Lipid 73, 159–180.
[14] Lundbæk, J.A., Birn, P., Girshman, J., Hansen, A.J. and Andersen, O.S. (1996) Biochemistry 35, 3825–3830.
[15] Sarges, R. and Witkop, B. (1965) J. Am. Chem. Soc. 87, 2011–2019.
[16] Arsen'ev, A.S., Barsukov, I.L., Bystrov, V.F., Lomize, A.L. and Ovchinnikov, Y.A. (1985) FEBS Lett. 186, 168–174.
[17] O'Connell, A.M., Koeppe II, R.E. and Andersen, O.S. (1990) Science 250, 1256–1259.
[18] Koeppe, R.E. and Andersen, O.S. (1996) Annu. Rev. Biophys. Biomol. Struct. 25, 231–258.
[19] Hladky, S.B. and Haydon, D.A. (1970) Nature 225, 451–453.
[20] Elliott, J.R., Needham, D., Dilger, J.P. and Haydon, D.A. (1983) Biochim. Biophys. Acta 735, 95–103.
[21] Busath, D., Andersen, O.S. and Koeppe II, R.E. (1987) Biophys. J. 51, 79–88.
[22] Veatch, W.R. and Blout, E.R. (1974) Biochemistry 13, 5257–5264.
[23] Durkin, J.T., Providence, L.L., Koeppe II, R.E. and Andersen, O.S. (1992) Biophys. J. 62, 145–159.
[24] Chupin, V., Killian, J.A. and De Kruijff, B. (1987) Biophys. J. 51, 395–405.
[25] Killian, J.A. (1992) Biochim. Biophys. Acta 1113, 391–425.
[26] Andersen, O.S. (1983) Biophys. J. 41, 119–133.
[27] Andersen, O.S. and Koeppe II, R.E. (1992) Physiol. Rev. 72, S89–S158.
[28] Veatch, W.R. and Blout, E.R. (1974) Biochemistry 13, 5257–5264.
[29] Roux, B., Brueschweiler, R. and Ernst, R.R. (1990) Eur. J. Biochem. 194, 57–60.
[30] Killian, J.A., Prasad, K.U., Urry, D.W. and De Kruijff, B. (1989) Biochim. Biophys. Acta 978, 341–345.
[31] Mattice, G.L. (1993) Ph.D. Thesis, Department of Chemistry and Biochemistry, University of Arkansas.
[32] Greathouse, D.V., Hinton, J.F., Kim, K.S. and Koeppe II, R.E. (1994) Biochemistry 33, 4291–4299.
[33] Starling, A.P., East, J.M. and Lee, A.G. (1995) Biochem. J. 308, 343–346.
[34] Huang, H.W. (1995) J. Phys. II France 5, 1427–1431.